

Spectral Mixture Decomposition by Least Dependent Component Analysis

Sergey A. Astakhov^{a,*}, Harald Stögbauer^a,
Alexander Kraskov^{a,b}, Peter Grassberger^a

^a*John von Neumann Institute for Computing, Forschungszentrum Jülich,
D-52425, Jülich, Germany*

^b*Division of Biology, California Institute of Technology, Pasadena, CA 91125,
USA*

Abstract

A recently proposed mutual information based algorithm for decomposing data into least dependent components (MILCA) is applied to spectral analysis, namely to blind recovery of concentrations and pure spectra from their linear mixtures. The algorithm is based on precise estimates of mutual information between measured spectra, which allows to assess and make use of actual statistical dependencies between them. We show that linear filtering performed by taking second derivatives effectively reduces the dependencies caused by overlapping spectral bands and, thereby, assists resolving pure spectra. In combination with second derivative preprocessing and alternating least squares postprocessing, MILCA shows decomposition performance comparable with or superior to specialized chemometrics algorithms. The results are illustrated on a number of simulated and experimental (infrared and Raman) mixture problems, including spectroscopy of complex biological materials.

Key words: multivariate curve resolution, independent component analysis (ICA), mutual information, MILCA, nonnegativity

1 Introduction

The problem of estimating parameters (concentrations and pure spectra) of a linear mixture model underlying a set of spectroscopic measurements has spurred growth of more than 20 algorithms [1] that now form an arsenal known

* Corresponding author: Tel.: +49 2461 612526; Fax: +49 2461 612430.
Email address: s.astakhov@fz-juelich.de (Sergey A. Astakhov).

as multivariate self-modeling curve resolution tools (for recent reviews see [2,3,4,5,6,7,8]). Although advanced to the point that they have been implemented as commercial software (e.g., [9,10,11,12]), these techniques still leave room for new developments [13,14,15].

In their pioneering work, Lawton and Sylvestre [16] proposed decomposition of mixed spectral signals into *independent* pure components. In practice, this will not be feasible, since different chemical species do not necessarily have completely independent spectra (e.g., because they may contain identical or similar functional groups). Thus, any residual statistical dependencies in the recovered sources might either signal a failure of the method, or reflect the fact that the goal of achieving independent spectra was inconsistent. Aside from that, there have been only relatively few separate attempts [17,18,19,20,21,22,23,24,25,26,27,28,29,30,31] to use statistical (in)dependence of recovered sources (measured, e.g., by *mutual information* [32]) as a criterion in multivariate curve resolution. However, a more systematic study of applicability of these methods in spectral analysis is due.

Viewed in a broader context, the use of these statistical dependencies constitutes the basis for the rapidly growing field of Independent Component Analysis (ICA) or, more generally, Blind Source Separation (BSS) [33,34,35,36,37,38,39,40,41]. One of the characteristic features of multivariate spectral curve resolution is that in most spectroscopic techniques the instrumental signals are nonnegative. In ICA or BSS, sources are not generally assumed to be of definite sign, although there are a number of papers in the BSS literature [42,43,44,45,46,47] that deal specifically with nonnegative sources. Clearly, such methods capable of efficient decomposing nonnegative mixtures can be of potential use in analytical practice.

The ICA approach rests on the underlying assumption of statistical independence of original (pure) sources [38,39]. In such a case pure signals can be recovered by finding a demixing transformation that minimizes dependencies between estimates. If the original independent sources and concentrations are positive, then also the estimates should be so [45] and nonnegativity can be used as a test of decomposition. Alternatively, nonnegativity may serve as a target property in optimization, together with other properties such as maximal independence (see, for example, the *Nonnegative PCA* algorithm [46] and several chemometrics techniques that use the nonnegativity constraint [1,11,14,15,16,48,49]).

As we already pointed out, in realistic problems the original spectral signals are not perfectly independent (“overlapping bands”). These dependencies originate from similarities in the chemical structure, e.g., due to the presence of similar functional groups. Such mixtures are typically hard to decompose. This raises difficulties in straightforward use of general purpose ICA algorithms [49],

which can only be studied by detailed simulations. Here we present a comparative study based on extensive statistics and show how the ICA methodology applies to realistic chemometrics problems.

In spectral analysis, the overlap problem has motivated the development of specialized curve resolution methods. For instance, one group of algorithms is based on the idea of “pure variables” [50]. A “pure variable” is a wavelength at which only one of the components contributes. Isolation of pure variables for all mixture components is then a key to decomposition. This way to avoid the problem of overlapping bands was successfully implemented in several algorithms, e.g., KSFA [51], SIMPLISMA [9], IPCA [52] and, more recently, SMAC [53]). Also, *Band-Target Entropy Minimization* (BTEM [15,54]) has been proposed which involves an explicit (made by visual inspection [15]) choice of spectral features (target regions) to be retained in the course of constrained optimization. While efficient and highly flexible, supervised band selection has the drawbacks of being neither fully automated nor completely blind [2].

Since ICA is in most applications confronted with signals that cannot be linearly decomposed into independent sources, a more proper name would in such cases be the “Least dependent Component Analysis”. Analyzing dependencies between reconstructed sources should then be an integral part of the method. A technical problem for such an analysis has been the need for fast, robust, precise and bias free estimators for mutual information (MI). In a recent paper we employed a novel MI estimator with notably improved properties [55] in what we called the *Mutual Information based Least dependent Component Analysis* (MILCA [56]). MILCA combines several features: (i) high performance ICA algorithm; (ii) output reliability tests; (iii) cluster analysis of reconstructed sources for residual interdependencies; and (iv) joining highly dependent sources into multi-dimensional sources. It has been extensively tested and compared to other ICA algorithms on various blind separation problems. MILCA was found to outperform existing algorithms based on cruder approximations of mutual information (or other measures of independence) [56]. Some of those, e.g., FastICA [17,18,19,20,21,22,23,24,25,26,35], JADE [20,27,28,40], Infomax [29,41], SOBI [31,36] had been employed in the earlier applications of ICA to spectral curve resolution. These results suggest that further progress in developing high-performance ICA methods may well determine their place in practical analytical spectroscopy.

In this paper we study the potential of MILCA, assisted by proper data pre-processing and postprocessing, in model-free blind spectral curve resolution. Unlike specialized chemometrics techniques, MILCA does not make use of nonnegativity, nor does it rely on band selection in any form. One could of course include violations of nonnegativity in some way as a contribution to the cost function (which would otherwise be just the mutual information) to

be minimized. However, we will not do this here, partly because it is not *a priori* clear how to weigh these two contributions. Instead, the present study elaborates on how violations of nonnegativity correlate with the quality of decomposition, and we will make direct comparisons with other chemometrics algorithms.

The paper has the following structure. Section 2 introduces our approach to computing mutual information. It gives a description of the MILCA algorithm along with the preprocessing, optional corrections for residual negativity (postprocessing) and measures of performance used. In Section 3 the data sets analyzed in this work are briefly described. Section 4 concentrates on main results and, finally, conclusions are in Section 5.

2 Methods

2.1 Mutual information

For a multivariate continuous random variable (X_1, X_2, \dots, X_M) with given marginal and joint densities $\mu_i(x_i)$ and $\mu(x_1, x_2, \dots, x_M)$, the mutual information is given by [32,55,56,57]

$$I(X_1, X_2, \dots, X_M) = \sum_{i=1}^M H(X_i) - H(X_1, X_2, \dots, X_M), \quad (1)$$

where

$$H(X_i) = - \int \mu_i \ln \mu_i dx_i \quad (2)$$

and

$$H(X_1, X_2, \dots, X_M) = - \int \mu \ln \mu dx_1 dx_2 \dots dx_M \quad (3)$$

are the differential entropies [32].

The MI is a measure of statistical dependence of the M variables, which means that it is zero if they are strictly independent (i.e., their joint density factorizes, $\mu = \prod_i \mu_i$), and it is positive otherwise. The advantages of MI is that it is sensitive to all types of dependencies (while, e.g., Pearson's coefficient is sensitive only to linear correlations) and it has a well defined information theoretic meaning. Also, due to the *grouping property* [55], it can

be decomposed for any partitioning of the set $\{X_1, X_2, \dots, X_M\}$ into dependencies within groups of X_i and dependencies between these groups, e.g., $I(X_1, X_2, X_3) = I(X_1, X_2) + I((X_1, X_2), X_3)$. This leads directly to a conceptually extremely simple method of mutual information based hierarchical clustering (MIC [57]).

When the variables X_i represent experimental measurements, information about them is usually given by a finite number of samples (realizations) x_i^k , $k = 1, 2, \dots, N$, and MI has to be estimated by statistical inference. In our present case, the raw data will be an $M \times N$ matrix \mathbf{X} of M spectra \mathbf{x}_i sampled at N wavelengths (frequencies) ν^k each

$$\mathbf{X} = \begin{pmatrix} x_1^1 & x_1^2 & \dots & x_1^N \\ x_2^1 & x_2^2 & \dots & x_2^N \\ \dots & \dots & \dots & \dots \\ x_M^1 & x_M^2 & \dots & x_M^N \end{pmatrix}. \quad (4)$$

Note that we view each spectrum as a random variable X_i ($i = 1, 2, \dots, M$) and the N spectral values x_i^k , $k = 1, 2, \dots, N$ as its realizations. This should be contrasted to the alternative point of view where each spectral value at a given frequency ν^k defines a random variable X_k , $k = 1, 2, \dots, N$, and x_i^k , $i = 1, 2, \dots, M$ are its realizations. Our task consists in computing (and subsequently minimizing) the MI estimator $\hat{I}(\mathbf{X})$ of the spectral data given by Eq. (4). Obviously, the realizations $\xi^k = (x_1^k, x_2^k, \dots, x_M^k)$ are not independent of each other, but in the following we shall neglect this and use estimators developed for independent identically distributed realizations.

The estimators given in [55] (which are actually closely related to the estimator for differential Shannon entropies used in [58]) are based on k -nearest neighbor statistics. They have been shown to give rather precise estimates of MI in any dimension M . In particular, they seem to be numerically free of bias for independent signals (when MI is zero). But even when this is not the case, their bias and variance seem to be smaller than those of other estimators [55].

2.2 Least dependent component approach

As in the basic multivariate curve resolution setting, linear ICA starts out with a mixture model in the form

$$\mathbf{X} = \mathbf{A}\mathbf{S}, \quad (5)$$

where \mathbf{X} is a $M \times N$ matrix of mixed signals, \mathbf{S} is a $K \times N$ matrix of unknown pure components ($\mathbf{s}_1, \mathbf{s}_2, \dots, \mathbf{s}_K$), and \mathbf{A} is an $M \times K$ mixing matrix (concentrations). The problem is to reconstruct blindly \mathbf{S} and \mathbf{A} from the observations \mathbf{X} , assuming that the original sources are as “independent” as possible. More precisely, the demixing transformation \mathbf{W} (which is an estimate for \mathbf{A}^{-1} with the superscript -1 denoting matrix inverse or pseudoinverse) is sought such that it minimizes the mutual information estimator $\hat{I}(\mathbf{Y})$ of the estimated components $\mathbf{Y} = \mathbf{W}\mathbf{X}$. The ICA decomposition is defined up to scaling (intensity ambiguity [59]) and permutation of sources [45]. In the simplest version of the MILCA algorithm which we apply here, the MI between components \mathbf{y}_i is computed at equal frequencies ν^k (possible dependencies between sources at different frequencies can be assessed, e.g., using “delay” vectors; for details on this technique and also for a noninstantaneous mixing ansatz see [56]).

The first step in ICA usually comprises principal component analysis (PCA), also called (pre)whitening [37,38,60] which minimizes linear correlations in the data. The number of sources ($K \leq M$) is estimated in PCA by taking only decorrelated components with highest eigenvalues. Then the demixing transformation splits into a $K \times M$ prewhitening matrix \mathbf{V} and a square rotation matrix \mathbf{R} :

$$\mathbf{W} = \mathbf{R}\mathbf{V}. \tag{6}$$

Thus, the ICA problem reduces to searching the minimum of $\hat{I}(\mathbf{Y})$ under pure rotation $\mathbf{Y} = \mathbf{R}\mathbf{Z}$ of prewhitened vectors $\mathbf{Z} = \mathbf{V}\mathbf{X}$. An important simplification comes from the fact that rotation matrix can be further decomposed into $\mathbf{R} = \prod_{i,j}^K \mathbf{R}_{i,j}$, where each two-dimensional rotation $\mathbf{R}_{i,j}$ acts on $(\mathbf{z}_i, \mathbf{z}_j)$ and is obtained so that it minimizes pairwise mutual information $\hat{I}(\mathbf{y}_i, \mathbf{y}_j)$. Convergence to the minimum of $\hat{I}(\mathbf{Y})$ is achieved once all $\mathbf{R}_{i,j}$ have been optimized iteratively (for implementation details we refer to [56]). Drawing a line to curve resolution methods, \mathbf{R} resolves rotational ambiguity [59] by bringing the estimates as close to the initial independence assumption as possible.

The use of proper preprocessing of data can significantly improve performance of curve resolution algorithms. Here we study how MILCA performs on second derivative (SD) spectral data which are known to be better suited for spectral analysis of complex mixtures [18,31,61,62] than original (raw) spectra. We will explain why such preprocessing improves ICA decomposition performance. Specifically, one proceeds from original mixture vectors \mathbf{X} to their second derivatives \mathbf{X}'' with respect to frequency (wavelength), approximated either by finite differences

$$\left. \frac{d^2x(\nu)}{d\nu^2} \right|_{\nu^k} \sim x(\nu^{k-1}) - 2x(\nu^k) + x(\nu^{k+1}), \tag{7}$$

or by means of smoothing polynomial Savitzky-Golay differentiation [63]. Then, PCA and MI minimization can be performed on \mathbf{X}'' , yielding \mathbf{W}'' and \mathbf{Y}'' (here and below double primes indicate quantities estimated using SD data, whereas superscript (0) will indicate estimates obtained in the original space). Due to linearity of Eqs. (5) and (7), \mathbf{W}'' represents an estimate for demixing matrix \mathbf{A}^{-1} . The estimates for pure spectra (in the original space) can be recovered by applying the demixing transformation \mathbf{W}'' on the original measured mixture signals

$$\mathbf{Y} = \mathbf{W}''\mathbf{X}. \quad (8)$$

The MILCA estimates for spectra \mathbf{Y} and concentrations $\tilde{\mathbf{A}} = (\mathbf{W}'')^{-1}$ can be further refined iteratively through an alternating least squares (ALS, [11,64]) procedure. In this method the nonnegativity constraint on spectra and concentrations is imposed in a postprocessing step (i.e., after mixture decomposition has been done by some curve resolution algorithm). Specifically, one can write the ALS iterations as follows:

- (1) set $j=0$; initialize $\tilde{\mathbf{Y}}_0 = \mathbf{Y}$, $\tilde{\mathbf{A}}_0 = \tilde{\mathbf{A}}$;
- (2) set negative entries of $\tilde{\mathbf{A}}_j$ to zero;
- (3) update spectra $\tilde{\mathbf{Y}}_{j+1} = (\tilde{\mathbf{A}}_j^T \tilde{\mathbf{A}}_j)^{-1} \tilde{\mathbf{A}}_j^T \mathbf{X}$ using the new (nonnegative) $\tilde{\mathbf{A}}_j$;
- (4) set negative entries of $\tilde{\mathbf{Y}}_{j+1}$ to zero;
- (5) update concentrations $\tilde{\mathbf{A}}_{j+1} = \mathbf{X} \tilde{\mathbf{Y}}_{j+1}^T (\tilde{\mathbf{Y}}_{j+1} \tilde{\mathbf{Y}}_{j+1}^T)^{-1}$ using the new (nonnegative) $\tilde{\mathbf{Y}}_{j+1}$;
- (6) $j = j + 1$; continue at (2) until convergence is reached;

We denote the result of ALS iterations by $\mathbf{Y}^{(a)}$ and $\mathbf{W}^{(a)}$. If initial $\tilde{\mathbf{Y}}_0$ and $\tilde{\mathbf{A}}_0$ are already close to the optimal solution, then the ALS procedure should give small corrections by eliminating the negativity of ICA estimates. Notice that the mutual information $\hat{I}(\tilde{\mathbf{Y}}_j)$ will in general slightly increase during the ALS postprocessing, although, as we will show below, the decomposition performance is in most cases considerably improved due to better fulfilled nonnegativity constraint.

2.3 Measures of performance

Bearing in mind the scaling and permutation ambiguities, a good quality measure for ICA results is the Amari error index [39,56,58], which quantifies how well the demixing transformation \mathbf{W} agrees with the true mixing matrix \mathbf{A} (if such is known)

$$P(\mathbf{W}, \mathbf{A}) = \frac{1}{2K} \sum_{i,j=1}^K \left(\frac{|p_{ij}|}{\max_k |p_{ik}|} + \frac{|p_{ij}|}{\max_k |p_{kj}|} \right) - 1, \quad (9)$$

where $p_{ij} = (\mathbf{WA})_{ij}$. The Amari index P vanishes if \mathbf{W} deviates from \mathbf{A}^{-1} only in scaling and permutation of elements, and it increases as the quality of decomposition becomes poor.

Other measures of decomposition performance are applied to match reconstructed components with pure original sources. To compare our results with those of [15], we shall use the inner product of normalized pure and estimated spectral vectors

$$i(\mathbf{y}, \mathbf{s}) = \frac{(\mathbf{y} \cdot \mathbf{s})}{|\mathbf{y}||\mathbf{s}|}. \quad (10)$$

In addition, we introduce a scaled overall measure of positivity of the K vectors \mathbf{y}_i forming the matrix \mathbf{Y}

$$\pi(\mathbf{Y}) = \frac{1}{K} \sum_{i=1}^K \frac{\sum_{j:y_{ij}>0} y_{ij}}{\sum_{j=1}^N |y_{ij}|}. \quad (11)$$

If all vectors are strictly positive, $\pi(\mathbf{Y}) = 1$, while it is less than one otherwise.

3 Spectral data

Four exemplary data sets (A through D) taken from the literature were chosen to evaluate the performance of MILCA on typical spectral curve resolution problems. These included both artificial and experimental mixtures with various number of components M , amount of data points N and quality (e.g., noise level, presence of experimental background, line widths). Our choice of test problems was largely dictated by two requirements, which we consider essential: (i) data are publicly available, were previously used for the purposes of method evaluation and can be assessed later by alternative methods; (ii) the number of test problems is large enough to generate statistics of performance.

3.1 Simulated 3-component mixtures (A)

To compose a statistically representative test set of randomized mixtures we first collected a pool of 99 experimental infrared absorption spectra in the range 550–3830 cm^{-1} (822 data points each) selected from the NIST database [65]. This set was designed to contain organic compounds having common structural groups (halogen-, alkyl-, nitro-substituted benzene derivatives, phenols, alkanes; alcohols, thiols, amines, esters), so that their spectra have multiple overlapping bands and are, thereby, mutually dependent. After that a

sample of 10000 random triples of three-component mixtures ($M = K = 3$) was constructed by randomly choosing normalized pure spectra from the pool and applying random mixing matrices \mathbf{A} . The resulting sample represents then a set of blind source separation problems on strictly positive strongly dependent sources.

3.2 Near-infrared data set (B)

The second separation problem was chosen from the publicly available database [66] which was established in [67] to facilitate evaluation and comparison of chemometrical methods. The near-infrared (1100 – 2500 nm, 700 data points per spectrum) test sample first analyzed by Windig and Stephenson [62,68] consists of 140 experimental mixtures of five pure solvents (methylene chloride, 2-butanol, methanol, dichloropropane, acetone). For this data set both the concentrations in each mixture and the reference spectra of the pure components are available. The fractional concentrations of the four mixture components were chosen from the set $\{10\%, 22.5\%, 35\%, 47.5\%, 60\%\}$. The fractional concentration of the fifth component were set to make the concentrations add up to 100% [62].

3.3 6-component infrared mixtures (C)

To compare MILCA directly with the BTEM algorithm we also analyze here the same data as those used in the original work of Widjaja *et al.* [15] taking 14 randomized experimental 6-component mixtures of toluene, *n*-hexane, acetone, 3-phenylpropionaldehyde (aldehyde), 3,3-dimethylbut-1-ene (33DMB), and dichloromethane (DCM) [69]. To test performance, we used also the reference (pure) spectra of these compounds given in [15] (all spectra are FT-IR in the range 950 – 3200 cm^{-1} with 5626 intensities). Notice that the authors of [15] measured and decomposed a set of 18 spectra (including the experimental background). For more technical details see the footnote [69].

3.4 Raman spectra of brain samples (D)

True blind source separation by MILCA was performed on the spectral data measured from human brain samples by Krafft *et al.* [70]. Taken from neurosurgical resection material, the normal brain tissues of white and gray matter were subject to near-infrared Raman microspectroscopy, as were also the tumor specimens of glioma (astrocytoma *WHO*3) and meningioma (*WHO*1) types. The selected range was 600 – 3500 cm^{-1} covered by 3282 wavelenghts.

For each of the 4 samples, 20 to 42 measurements had been made resulting in 117 spectra. While variability across the sample is small, spectroscopically resolved differences between the four distinct specimens are noticeable. This allows to attempt blind mixture decomposition taking all 117 spectra together to extract common least dependent components in each sample and estimate their average concentrations. These results obtained blindly by MILCA were subsequently compared to the same Raman spectra of four pure substances (protein albumin from bovine serum, lipids from bovine brain extract, cholesterol from lanoline, and water) which were used in [70], assuming that they approximate the main constituents of the brain tissues.

4 Results and discussion

In order to illustrate potential pitfalls arising from dealing with highly dependent spectral signals, we first ran MILCA on a simple synthetic 2-component mixture of *o*-xylene and *p*-xylene, two compounds with very similar molecular structures and highly overlapping spectra (the spectral data were taken from [65]). The distribution on Fig. 1a shows that prewhitening (PCA) of the initially strictly positive components already leads to decorrelated vectors that cannot be made positive by any further pure rotation. Typically, in cases like this, minimizing the MI results in one component being poorly resolved, in appreciable violations of positivity and deviations from the pure signal itself (Figs. 1b,d). Obviously, this is even more severe for higher dimensional mixtures. It is therefore likely that in a problem with originally nonnegative overlapping sources already the first step (prewhitening) may be counterproductive. This may be the reason why algorithms based on PCA followed by subsequent rotation of decorrelated vectors into the positive domain (e.g., [46]) have so far met with limited success only (see also [49]). Likely, ICA approaches free of prewhitening might be more “compatible” with such strong constraints as nonnegativity.

When performing ICA in derivative space, the nonnegativity of components reconstructed by means of Eq. (8) is much better preserved (see Figs. 1c,e and figures shown below). The main reason for the improvements is that preprocessing with second derivatives removes slowly varying components from the spectra, and it is these slowly varying components which show most of the undesired dependencies between pure spectra. Seen from this point of view, discarding slow components in any multi-resolution decomposition such as, e.g., a wavelet decomposition [71] would presumably have similar effect as taking second derivatives (notice that we speak here of wavelets in the frequency space, not in the time domain). This is opposed to selecting nonoverlapping bands which would correspond to discarding spectral regions. Indeed, one might apply both techniques (band targeting and filtering out slow components) in

combination, but we shall not do this in the present paper.

We next studied behavior of MILCA (with and without (pre/post)preprocessing) on a large sample of synthetic randomized 3-component mixtures (data set A). To demonstrate the effect of SD preprocessing, Fig. 2a shows the mutual information of original triples of sources and those after taking second derivatives (Eq. (7)). There is a clear trend towards lowering MI by SD preprocessing. This means that taking derivatives filters out mostly the information which is common to all 3 spectra, and which is, therefore, detrimental to MILCA. Since SD acts as a high-pass filter, the effect can be traced to amplifying rapidly varying components. The observed gain in decomposition performance can be further understood by noting that the MI of estimated components is closer to the MI of pure components, if MILCA is performed in derivative space (Figs. 2b,c). Finally, Fig. 2d confirms that the match between MI of reconstructed signals and MI of original signals (both estimated in the original space) improves when SD preprocessing is involved (compare to Fig. 2c).

A more direct measure of performance (or quality of decomposition) is given by the degree to which the estimated demixing transformation corresponds to the actual mixing matrix and how well the nonnegativity is preserved. For this we gathered the statistics of the Amari index P (Eq. (9)) and positivity measure π (Eq. (11)) over the same test set A. As expected, the decomposition becomes more difficult as the sources become more dependent. But while this is very pronounced when MILCA is performed in the original space (Fig. 3a), it is hardly visible when second derivatives are used (Fig. 3b). In fact, MILCA with SD preprocessing was able to reconstruct successfully most of spectra from set A (Figs. 3d,f), in contrast to MILCA without SD preprocessing (Figs. 3c,e). Amari index values $P < 0.1$ indicate good decomposition quality, whereas $P > 0.3$ can be considered as unacceptable. Somewhat surprisingly, the strong (and expected) correlation between Amari index and nonnegativity seen when MILCA is done without filtering (Fig. 3e) is nearly completely eliminated with SD preprocessing (Fig. 3f). Again, this suggests that nonnegativity alone may not be the optimal target in a PCA-based spectral curve resolution.

In the following applications to experimental mixtures we will only use MILCA with second derivative preprocessing.

In order to see if postprocessing might further improve decomposition performance, we applied ALS with nonnegativity constraints (as described in Sec. 2.2, making 600 iterations for each mixture). Figure 4a shows that in the vast majority of cases the ALS corrections reduced the errors in mixture resolution and there was only a handful of mixtures (hardly seen in Fig. 4a), for which ALS iterations diverged far from the MILCA estimates and from the true solutions. The statistics of decomposition efficiency of the combination second derivatives-MILCA-ALS is notably improved, with the peak in

the Amari index distribution shifted down to $P \sim 0.05$ (Fig. 4b) which is indicative of a reliably high performance.

We now proceed to experimental mixture problems and comparisons with several chemometrics algorithms.

The test problem B offered a large set of mixtures to be decomposed, while each spectrum was relatively scarce in the number of data points (wavelengths). The five components have strong overlaps in the most informative range 2000–2500 nm (see Fig. 5), with only a few spectral features (also partly overlapping) at lower wavelengths to facilitate decomposition. Since the signals appeared rather smooth without much measurement noise, we performed MILCA on second derivatives computed by finite differences (Eq. (7)) (we verified that Savitzky-Golay smoothing did not improve results in this case). The resolved components were found to match the reference spectra fairly well with only minor violations of nonnegativity. The largest mismatches are observed for methylene chloride and 2-butanol (Figs. 5a,c).

To test how well the original concentrations were recovered, in the right panels of Fig. 5 we plot the estimated concentrations versus the original ones. Since the original concentrations were nearly quantized (see Sec. 3.2 and [62]), the vertical scatter of each point cloud indicates the inaccuracies of the source reconstruction. They are slightly larger than those obtained in [62] with SIMPLISMA, but MILCA produced notably fewer false negative concentrations: they occurred only for methylene chloride and 2-butanol (Figs. 5b,d) which show also the worst spectral reconstruction (Figs. 5a,c).

The next comparison was made with the BTEM algorithm [15,54]. For this we used the same data (set C) as in [15]. The large number of data points per spectrum and cleanness of the data even without background subtraction [69] allowed to work with second derivatives. In this case a Savitzky-Golay filter with 81 point window and 7th order polynomial gave best performance. Figure 6 depicts the resolved components plotted together with the reference (pure) spectra. Although the MILCA approach does not specifically focus on preserving certain spectral features, we find all the major bands reproduced reasonably well. Some distortions appear mostly in the overlap range 2800 – 3200 cm^{-1} which was also a source of imperfections in the BTEM analysis [15]. In Table 1 we give a quantitative comparison between SIMPLISMA, BTEM, and MILCA, with the inner product i (Eq. (10)) used as performance measure. Compared to BTEM, MILCA without ALS demonstrates almost equally high performance while being more straightforward in not using band selection. However, on this data set the combination of SIMPLISMA and ALS [9,11] evidently outperformed both. On the other hand, as reported in [15], the IPCA [52] and OPA [72] algorithms were less efficient. We find that MILCA+ALS performs clearly better than BTEM and is close in efficiency to

SIMPLISMA+ALS, although much more statistics would be needed to reliably judge the relative capabilities of these algorithms.

Finally, we proceed to a more realistic, true blind source separation problem in which no exact information on chemical composition is known. As non-invasive spectroscopic methods are more and more used in the analysis of biological materials and *in vivo* measurements [19,21,26,27,44,70,73,76], they offer an increasing variety of such “black” [2] mixture separation problems. Here we analyze the results of a Raman spectroscopy study of brain specimens [70] (set D) to see whether MILCA decomposition could be helpful in quantifying the abundances of major chemical species present in the brain. In [70] it was shown that a 4-component model can be used to explain a large part of the complex Raman spectra from brain samples. In their work Krafft *et al.* [70] assumed that the main spectral contributions are that of proteins, lipids, cholesterol and water, for which reference spectra were obtained. Then they determined concentrations of these components by making a linear fit to the experimental data. We attempted to do the same in a blind manner, applying MILCA to the original experimental set of spectra. The decomposition was complicated by the high level of measurement noise (Fig. 7a), so Savitzky-Golay smoothing derivatives (19 point window, polynomials of order 7) were used to preprocess the data. The first four least dependent components resolved by MILCA are plotted in Figs. 7b-e (the fifth and higher order components contained predominantly noise). We found that each of them was indeed very similar to one of the spectra from the model set (dashed curves in Figs. 7b-e), which supports the result of [70] that the model set represents the main constituents of the tissues. In addition, MILCA gives also estimates for the mixing matrices, i.e., for the concentrations. Based on these, we found the following lipid-to-protein average concentration ratios: 6.5 (white matter), 1.2 (gray matter), 0.5 (astrocytoma), and 0.4 (meningioma). This trend may be of diagnostic value and is consistent with the model fit parameters of [70] and with the studies by alternative methods [74,75,76].

5 Conclusions

We have approached several spectral curve resolution problems by a new blind source separation algorithm based on accurate estimates of mutual information (MILCA, available online at [77]). We showed that, with proper (pre/post)processing, decomposition into least dependent components is sufficient to achieve separation performance comparable to that of the state-of-the-art specialized chemometrics techniques.

Least dependent component analysis is a general statistical method with a very wide range of potential applications (here we refer to the extensive ICA liter-

ature surveyed, e.g., in [38,39]). It was designed to perform completely blindly without using any *a priori* or empirical information such as the locations of pure variables or nonnegativity of original sources. An important advantage of MILCA over other ICA methods is the fact that it can use (in)dependencies down to very small scales. Thus it can make efficient use of high pass filtered signals where most of the dependencies due to overlapping bands have been reduced. In practice, this may be helpful, e.g., in cases when reliable localization of pure variables is complicated by severe overlaps or noise. Also, opposite to the methods that actually rely on nonnegativity, MILCA is applicable to alternating sign signals, as is the case, e.g., in the EPR spectroscopy [22].

As our simulations on a large data set (10000 mixtures) have shown, the use of properly chosen preprocessing (second derivatives) leads to reduction of nuisance dependencies which would otherwise give unwanted contributions to mutual information. The latter is the only cost function in our method. In this sense, filtering out slowly varying contributions is consistent with the goal of finding least dependent components in the data performed by minimizing their mutual information.

Statistics of performance indicates also that imposing nonnegativity constraint during a postprocessing stage (e.g., in the form of alternating least squares) can further improve decomposition. We anticipate that the combination of MILCA and ALS will prove competitive in the category of PCA-based curve resolution algorithms.

The conceptual simplicity of the MILCA approach is expected to be advantageous in applied spectroscopy, and this contrasts it with novel but rather sophisticated curve resolution algorithms [15,54]. On the other hand, MILCA allows for several generalizations discussed already in [56]. These include mixing with small spectral shifts and testing the independence of spectra at different frequencies. In addition, it should be in principle feasible to include the nonnegativity constraint directly into the cost function.

However, more promising are algorithms based on stochastic (Monte Carlo type) minimization of mutual information subject to the nonnegativity constraint. The principal advantage of such methods is that if constrained minimization is performed under affine transformations (such as, e.g., combinations of rotations and shears [48,49]), then the prewhitening (PCA) and violations of nonnegativity it induces can be eliminated altogether. Our preliminary results (to be reported in a separate publication) indicate that the decomposition performance of these algorithms may be superior to their PCA-based counterparts.

Acknowledgements

We would like to thank Prof. D.L. Massart, Prof. P.K. Hopke for pointing us to the useful source [66] and Dr. W. Windig for the data set [68]. We appreciate cooperation of Prof. M. Garland, Dr. E. Widjaja who shared their spectra [15] and we thank Dr. C. Krafft for the original data from [70] and discussions. S.A. is grateful to Prof. S.P. Mushtakova and Dr. D.A. Smirnov for suggestions.

References

- [1] P.J. Gemperline, *Anal. Chem.* 71 (1999) 5398-5404.
- [2] Y.-Z. Liang, O.M. Kvalheim, R. Manne, *Chemometr. Intell. Lab. Syst.* 18 (1993) 235-250.
- [3] S.D. Brown, S.T. Sum, F. Despagne, B.K. Lavine, *Anal. Chem.* 68 (1996) 21R-61R.
- [4] P. Geladi, *Spectrochim. Acta B* 58 (2003) 767-782.
- [5] A. de Juan, R. Tauler, *Anal. Chim. Acta* 500 (2003) 195-210.
- [6] P.K. Hopke, *Anal. Chim. Acta* 500 (2003) 365-377.
- [7] B. Lavine, J.J. Workman, *Anal. Chem.* 76 (2004) 3365-3371.
- [8] T.-H. Jiang, Y. Liang, Y. Ozaki, *Chemometr. Intell. Lab. Syst.* 71 (2004) 1-12.
- [9] W. Windig, J. Guilment, *Anal. Chem.* 63 (1991) 1425-1432.
- [10] <http://www.acdlabs.com>
- [11] R. Tauler, B. Kowalski, S. Fleming, *Anal. Chem.* 65 (1993) 2040-2047.
- [12] <http://www.eigenvector.com>
- [13] M.N. Leger, P.D. Wentzell, *Chemometr. Intell. Lab. Syst.* 62 (2002) 171-188.
- [14] G. Peintler, I. Nagypal, I.R. Epstein, K. Kustin, *J. Phys. Chem. A* 106 (2002) 3899-3904.
- [15] E. Widjaja, C. Li, W. Chew, M. Garland, *Anal. Chem.* 75 (2003) 4499-4507.
- [16] W.H. Lawton, E.A. Sylvestre, *Technometrics* 13 (1971) 617-633.
- [17] D. Nuzillard, S. Bourg, J.M. Nuzillard, *J. Magn. Reson.* 133 (1998) 358-363.
- [18] J. Chen, X.Z. Wang, *J. Chem. Inf. Comput. Sci.* 41 (2001) 992-1001.
- [19] C. Ladroue, A.R. Tate, F.A. Howe, J.R. Griffiths, *Lect. Notes Comput. Sc.* 2412 (2002) 441-446.
- [20] S. Triadaphillou, A.J. Morris, E.B. Martin, in: *Proc. 4th International Symposium on Independent Component Analysis and Blind Signal Separation (ICA2003)*, Nara, Japan, 2003, pp. 879-884.
- [21] C. Ladroue, F.A. Howe, J.R. Griffiths, A.R. Tate, *Magnet. Reson. Med.* 50 (2003) 697-703.
- [22] J.Y. Ren, C.Q. Chang, P.C.W. Fung, J.G. Shen, F.H.Y. Chan, *J. Magn. Reson.* 166 (2004) 82-91.
- [23] X. Bi, T.H. Li, L. Wu, *Chem. J. Chinese Univ.* 25 (2004) 1023-1027.

- [24] M. Scholz, S. Gatzek, A. Sterling, O. Fiehn, J. Selbig, *Bioinformatics* 20 (2004) 2447-2454.
- [25] A. Pichler, M.G. Sowa, *J. Mol. Spect.* 229 (2005) 231-237.
- [26] F. Szabo de Edelenyi, A.W. Simonetti, G. Postma, R. Huo, L.M.C. Buydens, *Anal. Chim. Acta* 544 (2005) 36-46.
- [27] Y. Huang, P.J.G. Lisboa, W. El-Deredy, *Statist. Med.* 22 (2003) 147-164.
- [28] E. Visser, T.-W. Lee, *Chemometr. Intell. Lab. Syst.* 70 (2004) 147-155.
- [29] X.G. Shao, G. Wang, S. Wang, Q. Su, *Anal. Chem.* 76 (2004) 5143-5148.
- [30] H. Gao, T.H. Li, K. Chen, X. Bi, S.F. Lin, *Chinese J. Anal. Chem.* 32 (2004) 993-997.
- [31] N. Bonnet, D. Nuzillard, *Ultramicroscopy* 102 (2005) 327-337.
- [32] T.M. Cover, J.A. Thomas, *Elements of Information Theory*, Wiley, New York, 1991.
- [33] C. Jutten, J. Herault, *Signal Process.* 24 (1991) 1-10.
- [34] P. Comon, *Signal Process.* 36 (1994) 287-314.
- [35] A. Hyvärinen, E. Oja, *Neural Comput.* 9 (1997) 1483-1492.
- [36] A. Belouchrani, K. Abed-Meraim, J.-F. Cardoso, E. Moulines, *IEEE T. Signal Process.* 45 (1997) 434-444.
- [37] L. De Lathauwer, B. De Moor, J. Vandewalle, *J. Chemom.* 14 (2000) 123-149.
- [38] A. Hyvärinen, J. Karhunen, E. Oja, *Independent Component Analysis*, Wiley, New York, 2001.
- [39] A. Cichocki, S. Amari, *Adaptive Blind Signal and Image Processing. Learning Algorithms and Applications*, Wiley, New York, 2002.
- [40] J.-F. Cardoso, *Neural Comput.* 11 (1999) 157-192.
- [41] A.J. Bell, T.J. Sejnowski, *Neural Comput.* 7 (1995) 1129-1159.
- [42] D.D. Lee, H.S. Seung, *Nature* 401 (1999) 788-791.
- [43] G. Buchsbaum, O. Bloch, *Vision Res.* 42 (2002) 559-563.
- [44] P. Sajda, S. Du, L.C. Parra, in M.A. Unser, A. Aldroubi, A.F. Laine (Eds.), *Wavelets: Application in Signal and Image Processing X (SPIE Proc. Ser., Vol.5207)*, 2003, pp. 321-331.
- [45] A. Cichocki, P. Georgiev, *IEICE T. Fund. Electr. EA. E86A* (2003) 522-531.
- [46] M.D. Plumbley, E. Oja, *IEEE T. Neural Networ.* 15 (2004) 66-76.
- [47] Z.J. Yuan, E. Oja, *Lect. Notes Comput. Sc.* 3195 (2004) 1-8.

- [48] P. Paatero, U. Tapper, *Environmetrics* 5 (1994) 111-126.
- [49] P. Paatero, P.K Hopke, B.A. Begum, S.K. Biswas, *Atmospheric Environment* 39 (2005) 193-201.
- [50] F.J. Knorr, J.H. Futrell, *Anal. Chem.* 51 (1979) 1236-1241.
- [51] E.R. Malinowski, *Anal. Chim. Acta* 134 (1982) 129-137.
- [52] D.S. Bu, C.W. Brown, *Appl. Spectrosc.* 54 (2000) 1214-1221.
- [53] W. Windig, N.B. Galagher, J.M. Shaver, B.M. Wise, *Chemometr. Intell. Lab. Syst.* 77 (2005) 85-96.
- [54] L. Guo, F. Kooli, M. Garland, *Anal. Chim. Acta* 517 (2004) 229-236.
- [55] A. Kraskov, H. Stögbauer, P. Grassberger, *Phys. Rev. E* 69 (2004) 066138.
- [56] H. Stögbauer, A. Kraskov, S.A. Astakhov, P. Grassberger, *Phys. Rev. E* 70 (2004) 066123.
- [57] A. Kraskov, H. Stögbauer, R.G. Andrzejak, P. Grassberger, *Europhys. Lett.* 70 (2005) 278-284.
- [58] E.G. Learned-Miller, J.W. Fisher, *Journal of Machine Learning Research* 4 (2003) 1271-1295.
- [59] R. Tauler, A. Smilde, B. Kowalski, *J. Chemom.* 9 (1995) 31-58.
- [60] S. Wold, K. Esbensen, P. Geladi, *Chemometr. Intell. Lab. Syst.* 2 (1987) 37-52.
- [61] T.C. O'Haver, G.L. Green, *Anal. Chem.* 48 (1976) 312-318.
- [62] W. Windig, D.A. Stephenson, *Anal. Chem.* 64 (1992) 2735-2742.
- [63] A. Savitzky, M.J.E. Golay, *Anal. Chem.* 36 (1964) 1627-1639.
- [64] J.-H. Wang, P.K. Hopke, T.M. Hancewicz, S.L. Zhang, *Anal. Chim. Acta* 476 (2003) 93-109.
- [65] NIST Mass Spec Data Center. S.E. Stein, director, "Infrared Spectra" in NIST Chemistry WebBook, NIST Standard Reference Database Number 69, Eds. P.J. Linstrom and W.G. Mallard, March 2003, National Institute of Standards and Technology, Gaithersburg, MD, 20899 (<http://webbook.nist.gov>).
- [66] <ftp://clarkson.edu/pub/hopkepk>
- [67] P.K. Hopke, D.L. Massart, *Chemometr. Intell. Lab. Syst.* 19 (1993) 35-41.
- [68] W. Windig, *Chemometr. Intell. Lab. Syst.* 36 (1997) 3-16.
- [69] In [15], the authors analyzed 15 mixtures instead of 14 mixtures, although two of the spectra given in their data set (spectra #1 and #2) are identical. They also measured three background spectra with varying content of moisture and CO₂, bringing their total number of spectra to 18. They performed then the

BTEM analysis on all 18 spectra. However, since the background spectra are *known* to contain no contributions from the 6 mixture components of interest, it does not seem reasonable to treat them by any algorithm set up for *blind* source separation. Instead, in our analysis we first decomposed the background signals into three least dependent components (spectra of water, CO_2 and spectrometer background). After that these components were projected out by orthogonalizing in derivative space, and finally we performed MILCA on the 14 cleaned spectra. The results obtained in this way were practically the same as those from the most simple approach where we just neglected the background and did not do anything to minimize its effect. In view of this, in the following we discuss only the results obtained with the latter simple method.

- [70] C. Krafft, S. Miljanic, S.B. Sobottka, G. Schackert, R. Salzer, in: G.A. Wagnières, (Ed.), Diagnostic Optical Spectroscopy in Biomedicine II (SPIE Proc. Ser. Vol.5141), 2003, pp. 230-236.
- [71] L.B. Cao, P.D. Harrington, J.D. Liu, Anal. Chem. 77 (2005) 2575-2586.
- [72] F.C. Sánchez, J. Toft, B. van den Bogaert, D.L. Massart, Anal. Chem. 68 (1996) 79-85.
- [73] C. Krafft, Anal. Bioanal. Chem. 378 (2004) 60-62.
- [74] R. Campanella, J. Neurosurg. Sci. 36 (1992) 11-25.
- [75] A. Gaigneaux, C. Decaestecker, I. Camby, T. Mijatovic, R. Kiss, J.M. Ruyschaert, E. Goormaghtigh, Experimental Cell Research 297 (2004) 294-301.
- [76] C. Krafft, S.B. Sobottka, G. Schackert, R. Salzer, Analyst 130 (2005) 1070-1077.
- [77] <http://www.fz-juelich.de/nic/cs/software>

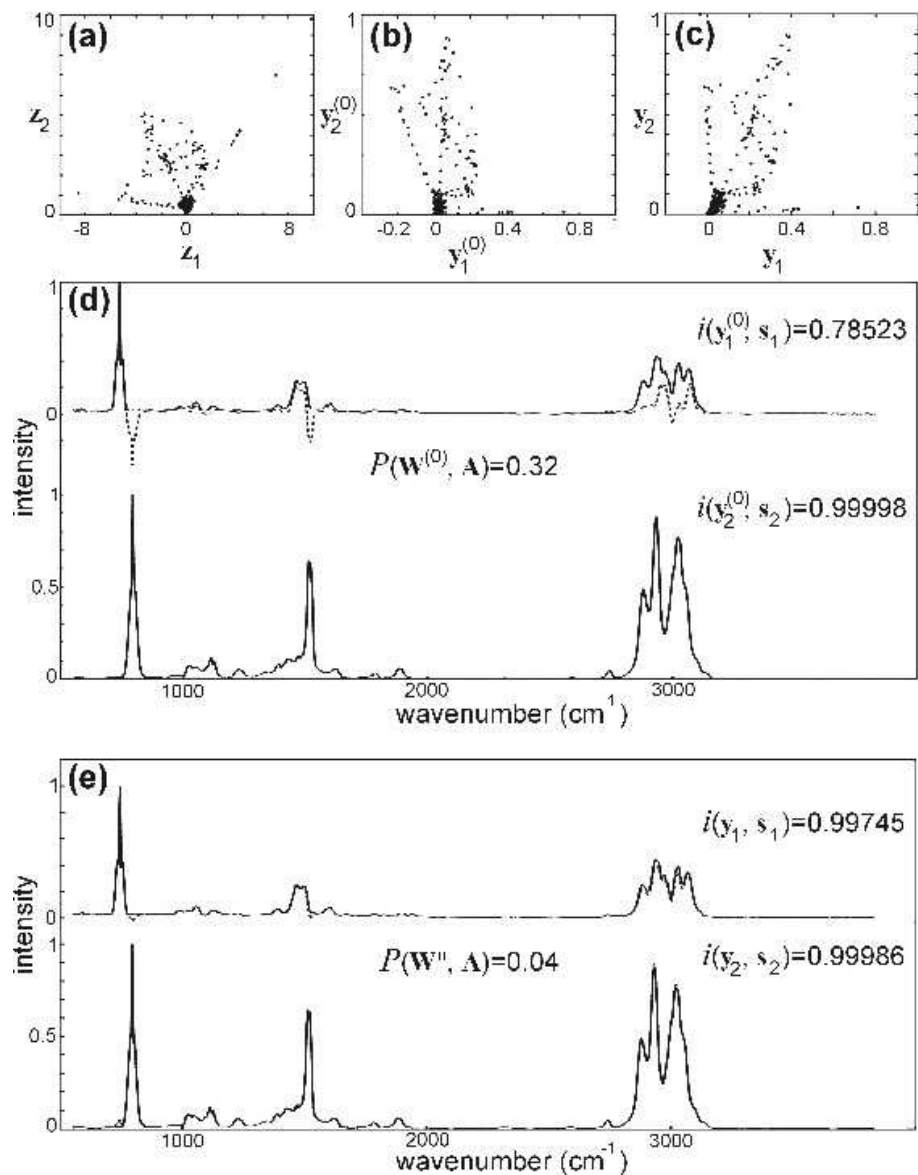


Fig. 1. PCA and MILCA applied to the mixture of *o*-xylene and *p*-xylene. Scatter plots of (a) PCA components z_1^k and z_2^k ($k = 1, 2, \dots, 822$) in the original space (\mathbf{z}_1 and \mathbf{z}_2), (b) ICA components ($y_1^{(0),k}$ and $y_2^{(0),k}$) reconstructed in the original space, (c) recovered components (y_1^k and y_2^k) with ICA done in SD space (see Eq. (8)). Panel (d) shows $\mathbf{y}_1^{(0)}$ (dashed curve) and the true pure spectra \mathbf{s}_1 and \mathbf{s}_2 (solid curves). The component $\mathbf{y}_2^{(0)}$ is indistinguishable from \mathbf{s}_2 . Panel (e) is the same for \mathbf{y}_1 and \mathbf{y}_2 obtained by MILCA in derivative space. In this case, the estimates are almost indistinguishable from the true sources. Also shown are the values of the inner product i (Eq. (10)) and the Amari index P (Eq. (9)).

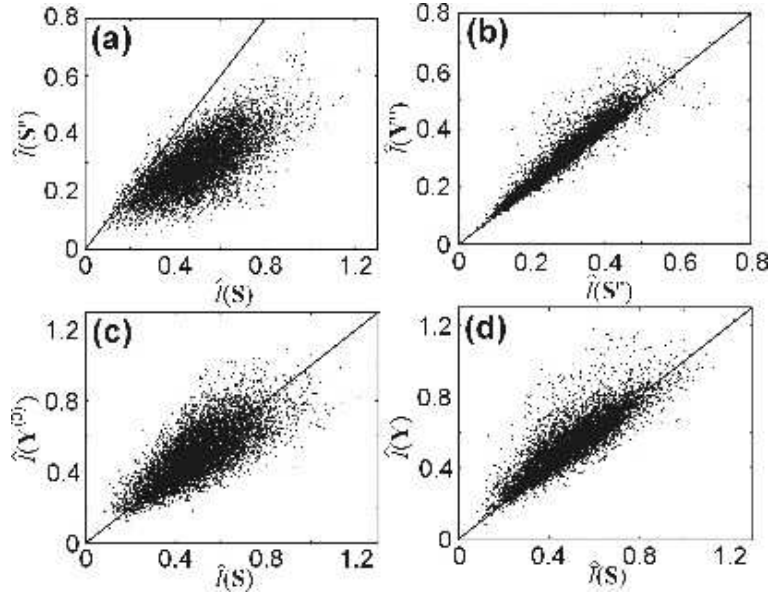


Fig. 2. Preprocessing and MILCA decomposition of 3-component mixtures (statistics over 10000 cases, data set A): (a) MI of the second derivatives of the sources \mathbf{S}'' plotted against MI of the original sources \mathbf{S} ; (b) MI of estimated SD spectra \mathbf{Y}'' against MI of the pure SD spectra \mathbf{S}'' ; (c) similar to panel (b), but without using second derivatives at all (MILCA is performed in the original space, producing estimates $\mathbf{Y}^{(0)}$); (d) again similar to panel (c), but with MILCA done using SD signals, in which case the estimates in the original space \mathbf{Y} are obtained through Eq. (8). Deviations from the straight lines indicate differences between quantities plotted on the vertical and horizontal axes.

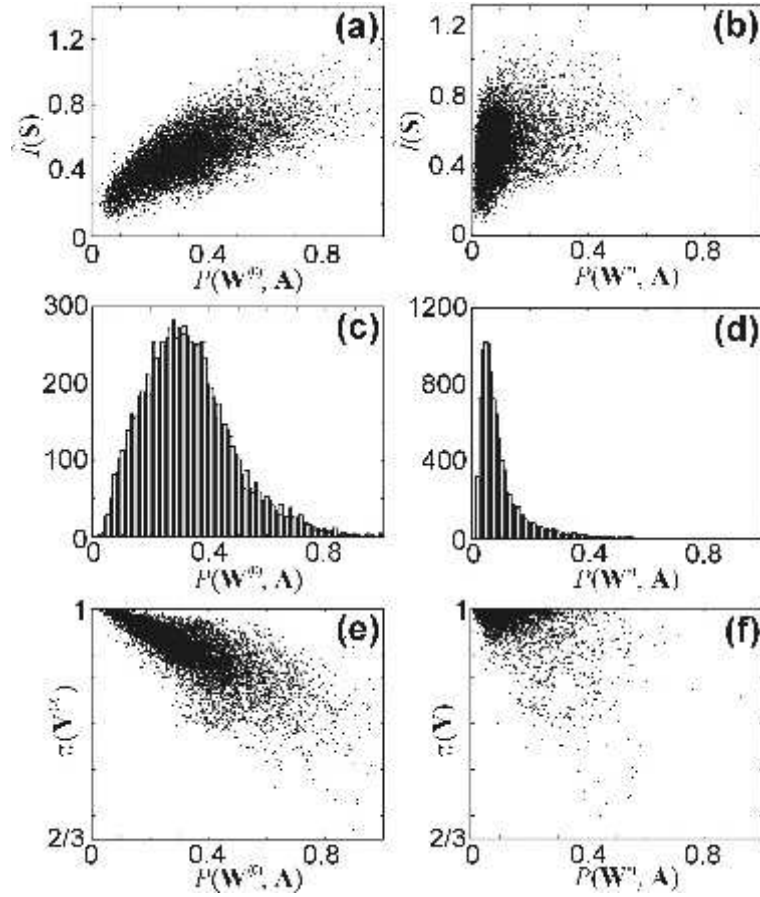


Fig. 3. MILCA performance statistics (10000 mixtures, data set A). Left (right) panels show results for MILCA in the original (second derivative) space: (a,b) MI of sources plotted against the Amari indices P (Eq. (9)) of the decompositions; (c,d) distributions of Amari indices over the test set; (e,f) dependence of the positivity measure π (Eq. (11)) on the Amari index P .

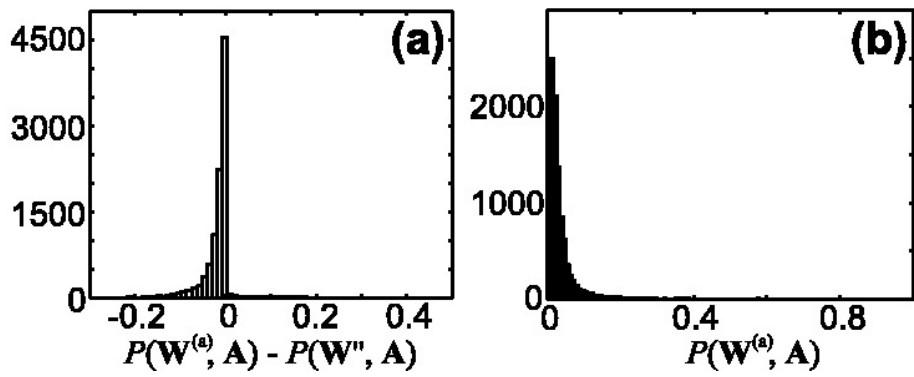


Fig. 4. Improvement in decomposition performance (a) and the resulting distribution (b) over the dataset \mathbf{A} achieved by applying the alternating least squares with nonnegativity constraint to the estimates from MILCA done in the second derivative space (to compare with Fig. 3d, same scale).

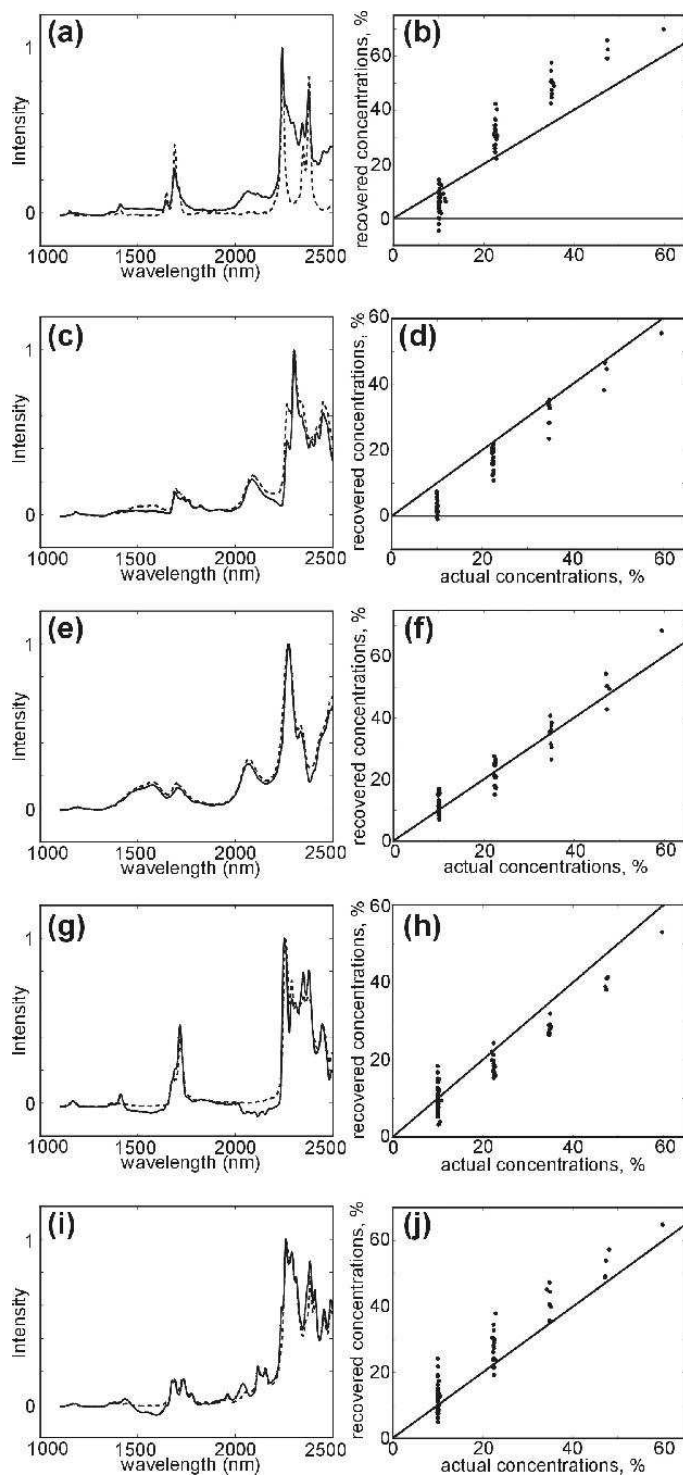


Fig. 5. Left column: Near-infrared spectra of estimated (solid curves) and original pure (dashed curves) components (data set B). The components were methylene chloride (a), 2-butanol (c), methanol (e), dichloropropane (g), and acetone (i). Right column: Estimated versus actual concentrations of these components. The straight lines have unit slopes and pass through the origin.

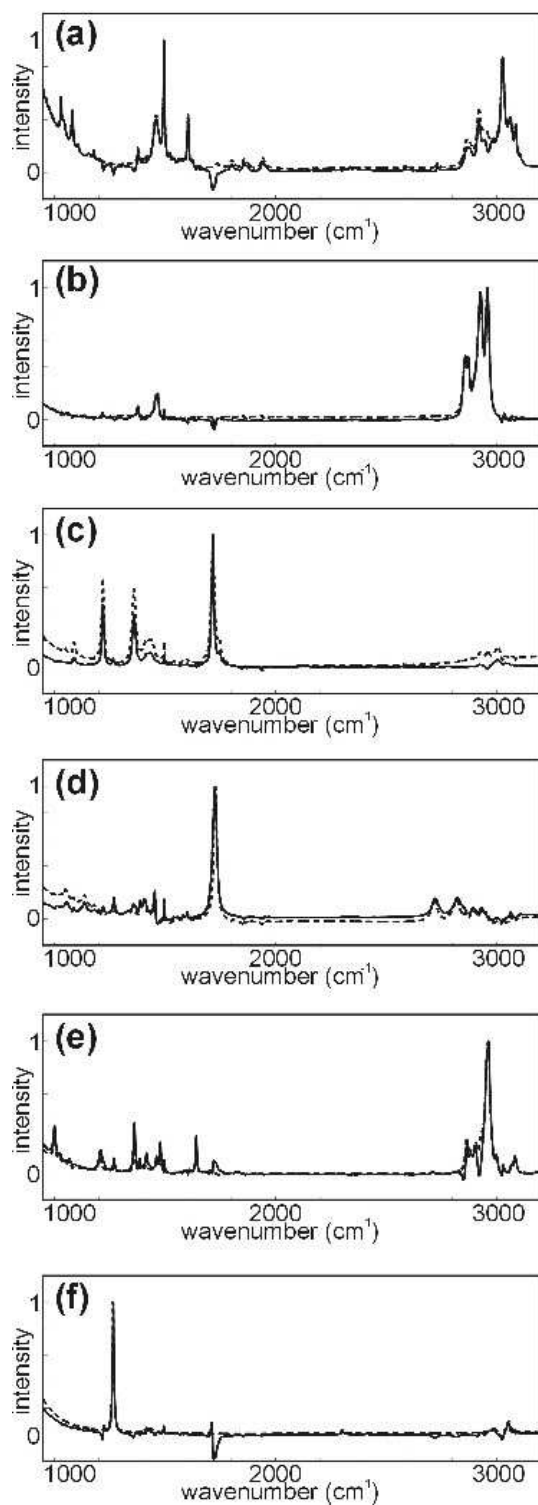


Fig. 6. Data set C: reconstructed by MILCA (solid) and reference [15] (dashed) spectra of toluene (a), *n*-hexane (b), acetone (c), aldehyde (d), 33DMB (e), DCM (f).

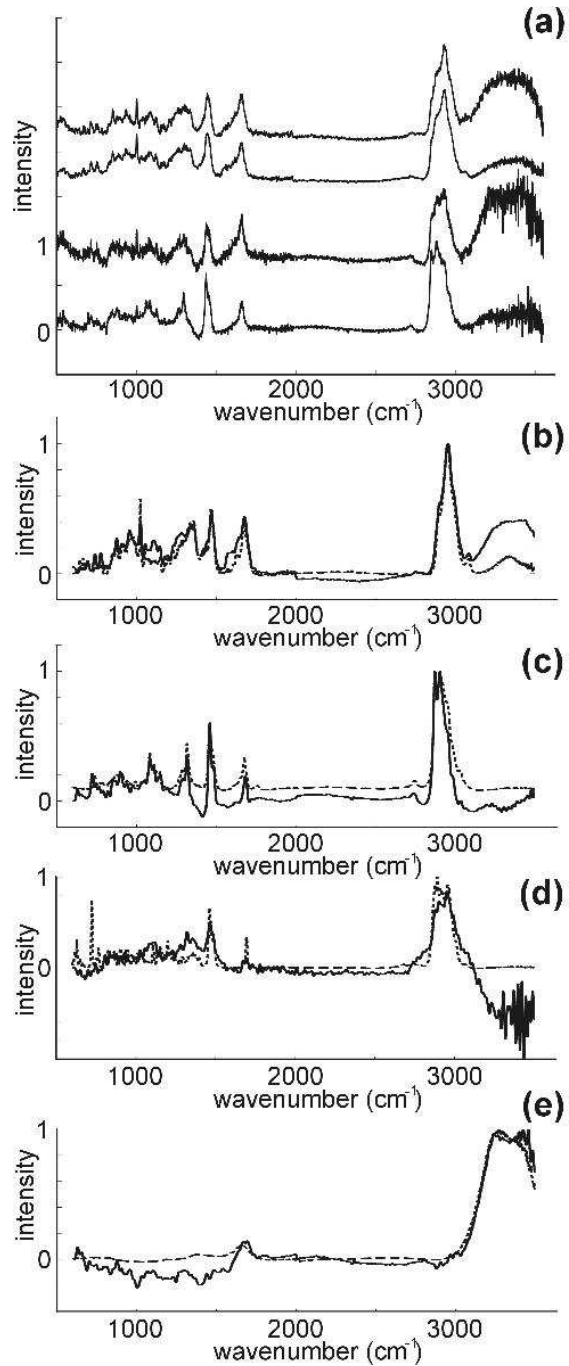


Fig. 7. Blind determination of composition of human brain tissue and tumors (data set D). Exemplary near-infrared Raman spectra (a) of normal white and gray matter, astrocytoma and meningioma tumors (from bottom to up). The four (b–e) estimated components (solid curves) plotted to compare with the model set (dashed curves) [70] consisting of protein (b), lipids (c), cholesterol (d) and water (e).

	SIMPLISMA	SIMPLISMA+ALS	BTEM	MILCA	MILCA + ALS
toluene	0.971	0.973	0.954	0.987	0.994
n-hexane	0.994	0.995	0.992	0.990	0.991
acetone	0.866	0.899	0.886	0.933	0.943
aldehyde	0.943	0.953	0.899	0.901	0.902
33DMB	0.576	0.963	0.983	0.964	0.948
DCM	0.969	0.967	0.904	0.909	0.966

Table 1

Data set C: performance of MILCA in comparison to the other curve resolution algorithms as measured by the values of inner product, Eq. (10), of reconstructed and reference spectra shown on Fig. 6. Numerical data for SIMPLISMA and BTEM were taken from Table 3 of [15].